Supporting Information for:

Interplay between hydrophilic and hydrophobic interactions in the self-assembly of a Gemini Amphiphilic Pseudopeptide: from vesicles to room temperature hydrogels

Jenifer Rubio,[a] Ignacio Alfonso [b,]* M. Isabel Burguete[a] and Santiago V. Luis [a,]*

[a]*Departamento de Química Inorgánica y Orgánica,Universidad Jaume I, Avd. Sos Baynat s/n, Castellón, Spain. Fax: +34 964728214; Tel: +34 964728239; E-mail: luiss@qio.uji.es*
[b]*Instituto de Química Avanzada de Cataluña, IQAC-CSIC, Jordi Girona 18-26, Barcelona, Spain. E-mail: ignacio.alfonso@iqac.csic.es*

Table of contents:

General experimental and synthetic procedures S-2
Copies of the NMR and ESI-MS spectra S-4
^{1}H NMR studies of in different solvents S-5
gNOESY spectrum of **1** S-6
gROESY spectrum of **1** S-7
DOSY spectrum of **1** S-8
Calculation of the cac S-9
SEM micrographs of **1** grown from different media S-10
SEM micrographs of compound **1** from different aqueous solutions S-11
TEM micrographs of compound **1** from different aqueous solutions S-12
TEM micrographs of **1** grown from different media S-13
Selected bands of the ATR FT-IR spectra of **1** at different conditions S-14
Procedure toward the formation of a stable gel at room temperature S-19
Photographs of gelation properties of **1** as a function of the gelator content (% wt) and the MeOH: H_2O proportion S-20
Photographs of gelation properties of **1** as a function of the EtOH: H_2O proportion S-22
Temporal stability of hydrogels S-22

General: Reagents and solvents were purchased from commercial suppliers (Adrich, Fluka or Merck) and were used without further purification. The precursor bis(amidoamine) was prepared as previously described.[1]

Electron microscopy: Scanning Electron Microscopy was performed either in a LEO 440I or in a JEOL 7001F microscope with a digital camera. Samples were obtained by slow evaporation of a solution (or a gel) of the compounds (~1-2 mg/ml) directly onto the sample holder, and were conventionally coated previous to the measurement. Transmission Electron Microscopy was carried out in a in a JEOL 2100 microscope at 120 KV. The micrographs were obtained from ~1 mg/ml solutions onto a holey carbon copper grid. The samples were sonicated for 10 minutes previous to the measurement, one drop added onto the grid and collected directly without staining.

NMR spectroscopy: The NMR experiments were carried out on a Varian INOVA 500 spectrometer (500 MHz for ^{1}H and 125 MHz for ^{13}C). Chemical shifts are reported in ppm using TMS as a reference.

Infrared spectroscopy: FT-IR spectra were acquired in a JASCO 6200 equipment having a MIRacle Single Reflection ATR Diamond / ZnSe accessory. We prepared a 20 mM sample of the corresponding pseudopeptide and we seeded it onto the ATR sample holder. We sequentially collected FT-IR spectra until the complete solvent evaporation.

Steady-state fluorescence spectroscopy: Steady-state fluorescence spectra were recorded in a Spex Fluorog 3-11 equipped with a 450 W xenon lamp. Fluorescence spectra were recorded in the front face mode. All the samples were measured in aerated conditions otherwise stated.
Gelation Test: The studied compound was dissolved in MeOH in a screw-capped cylindrical glass vial (diameter: 2 cm), the corresponding amount of water was added and the mixture was left at room temperature. A gel was considered to have formed when the soft material was stable upon turning the vial upside-down.

Calculation of the critical aggregation concentration (CAC) of compound 1: A series of aqueous solutions containing different concentrations of compound **1** (10^{-3} M – $10^{-6.3}$ M) were prepared. Each solution (2 mL) was mixed with a saturated pyrene solution (2 mL) and allowed to equilibrate (2 h). Steady state fluorescence spectra were recorded (λ_{exc} = 352 nm) and the ratio of the obtained I_1/I_3 was represented *vs.* the concentration of **1**.[2]

[1] J. Rubio, I. Alfonso, M. Bru, M. I. Burguete and S. V. Luis, *Tetrahedron Lett.*, 2010, **51**, 5861; J. Rubio, I. Alfonso, M. I. Burguete and S. V. Luis, *Soft Matter*, 2011, **7**, 10737.
[2] K. S. Sharma, C. Rodgers, R. M. Palepu and A. K. Rakshit, J. Colloid Interface Sci., 2003, 268, 482–488. T. Yoshimura, T. Ichinokawa, M. Kaji and K. Esumi, *Colloids Surf., A*, 2006, **273**, 208.

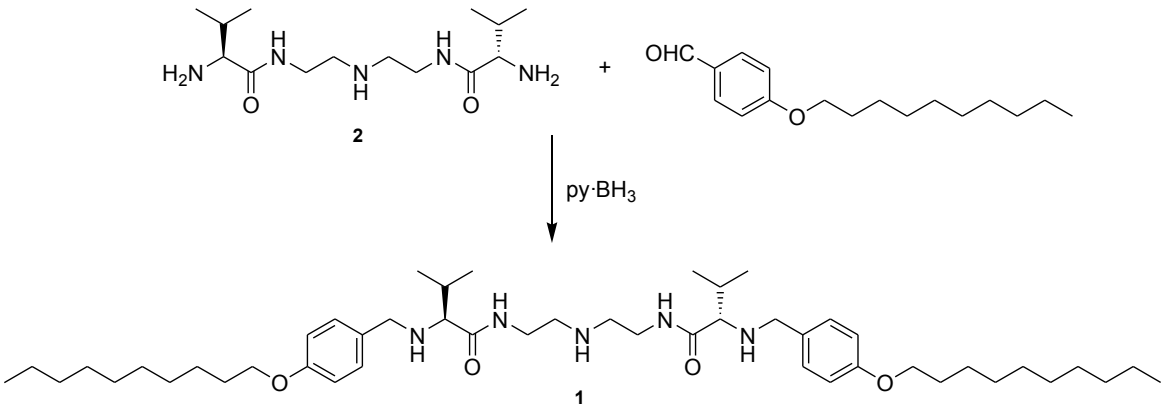

Synthesis of 1. The precursor bis(amidoamine) **2** (298.4 mg, 0.990 mmol) was dissolved in 10 mL of $CHCl_3$ and the solution was placed inside a flask under nitrogen atmosphere. 4-Decyloxybenzaldehyde (563.7 µL, 519.5 mg, 1.980 mmol) was dissolved in 5 mL of $CHCl_3$, this solution was added over the solution of **2** and then, 5 mL of $CHCl_3$ were added until a final volume of 20 mL (0.05 M final concentration each). The mixture was stirred overnight, then a large excess of py·BH_3 complex, 95% (1052.7 µL, 968.5 mg, 9.900 mmol) was carefully added at 35 ºC, and the mixture was allowed to react for 24 h before being hydrolyzed (conc. HCl, to acidity) and evaporated to dryness. The residue obtained was dissolved in water, basified with 1N NaOH, and extracted with $CHCl_3$. The combined organic layers were dried ($MgSO_4$) and evaporated in vacuum. The product was purified by flash chromatography on silica gel using CH_2Cl_2 as eluent, increasing slowly the polarity with MeOH and several drops of aqueous ammonia. Yield (472 mg, 60%); mp 79-81 ºC; $[\alpha]_D^{25}$ = -32.4 (c = 0.01, $CHCl_3$); IR (ATR) 3314, 2955, 2920, 2869, 2851, 1640, 1622, 1613, 1546, 1510 cm^{-1}; ^{1}H-NMR (500 MHz, $CDCl_3$) δ 0.88 (m, 12H), 0.93 (d, 6H, J = 6.9 Hz), 1.32 (m, 24 H), 1.44 (m, 4H), 1.76 (m, 4H), 2.07 (dtd, 2H, J = 4.8, 6.9, 13.8 Hz), 2.79 (t, 4H, J = 6.0 Hz), 2.94 (d, 2H, J = 4.6 Hz), 3.38 (dd, 4H, J = 5.9, 11.9 Hz), 3.55 (d, 2H, J = 12.9 Hz), 3.68 (d, 2H, J = 12.9 Hz), 3.93 (t, 4H, J = 6.6 Hz), 6.85 (d, 4H, J = 8.6 Hz), 7.19 (d, 4H, J = 8.6 Hz), 7.51 (t, 2H, J = 5.6 Hz); ^{13}C-NMR (125 MHz, $CDCl_3$) δ 14.1, 17.7, 19.6, 22.6, 26.0, 29.3, 29.3, 29.4, 29.5, 29.5, 31.3, 31.9, 38.7, 48.9, 52.8, 67.8, 68.0, 114.5, 129.3, 131.6, 158.4, 174.0; HRMS (ESI-TOF)$^+$ calc for $C_{48}H_{83}N_5O_4$ $(M + H)^+$: 794.6523; found 794.6532; Anal. Calcd. for $C_{48}H_{83}N_5O_4$: C, 72.59; H, 10.53; N, 8.82. Found: C, 72.45; H, 10.65; N, 8.94.

Figure S1. Spectral characterization of **1**: (A) ^{1}H NMR spectrum (500 MHz, 303 K, 20 mM in $CDCl_3$), (B) ^{13}C NMR spectrum (125 MHz, 303 K, 20 mM in $CDCl_3$), (C) Simulated (top) and experimental (down) HRMS (ESI^{+}-MS) of compound **1**.

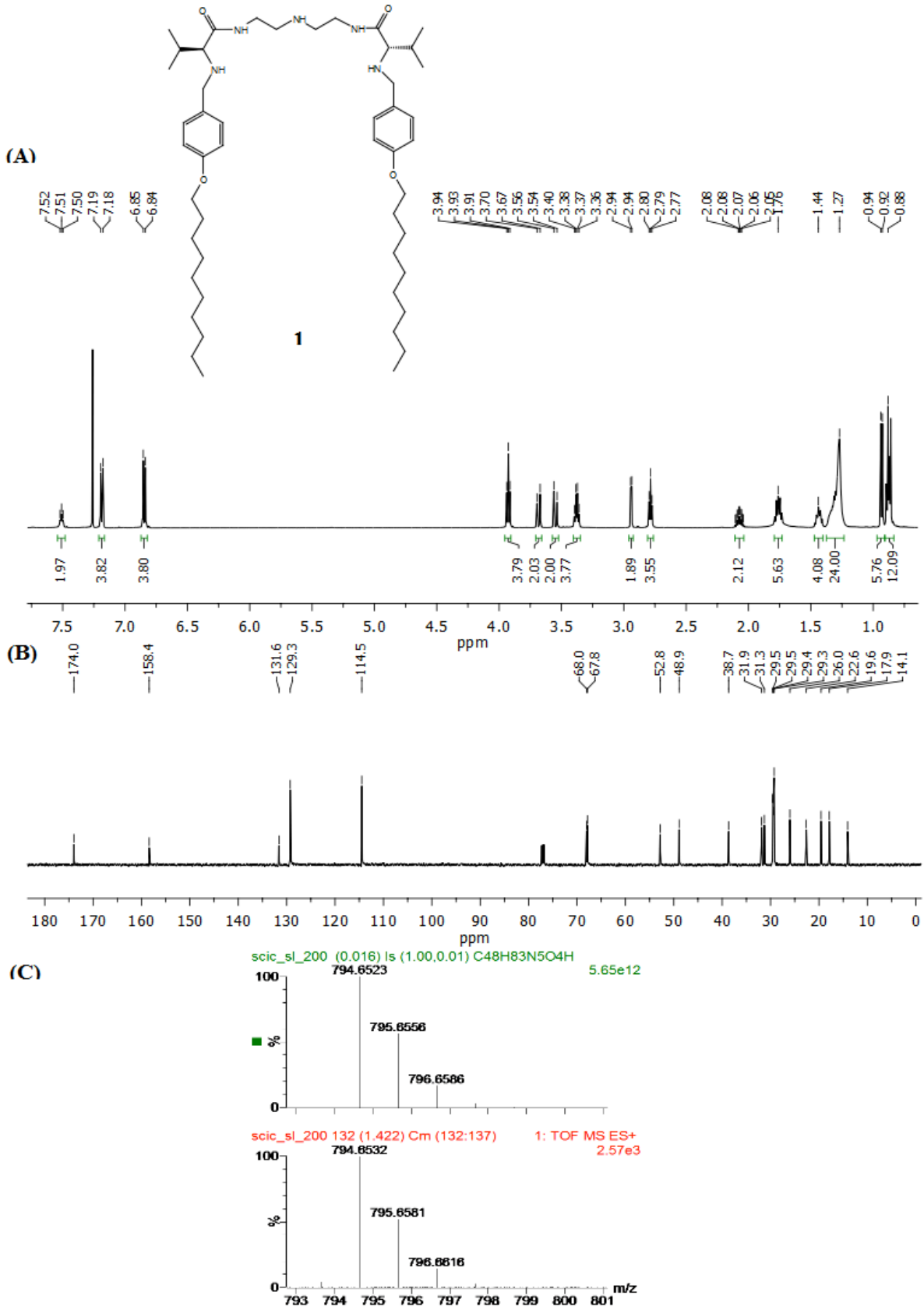

Figure S2. Comparison of the ^{1}H NMR spectra of **1** (500 MHz, 303 K) in different solvent compositions, from bottom to top:
(1) 20 mM of **1** in $CDCl_3$
(2) 20 mM of **1** in CD_3OD
(3) 20 mM of **1** in CD_3OD + acid
(4) 3 mM of **1** in D_2O + acid

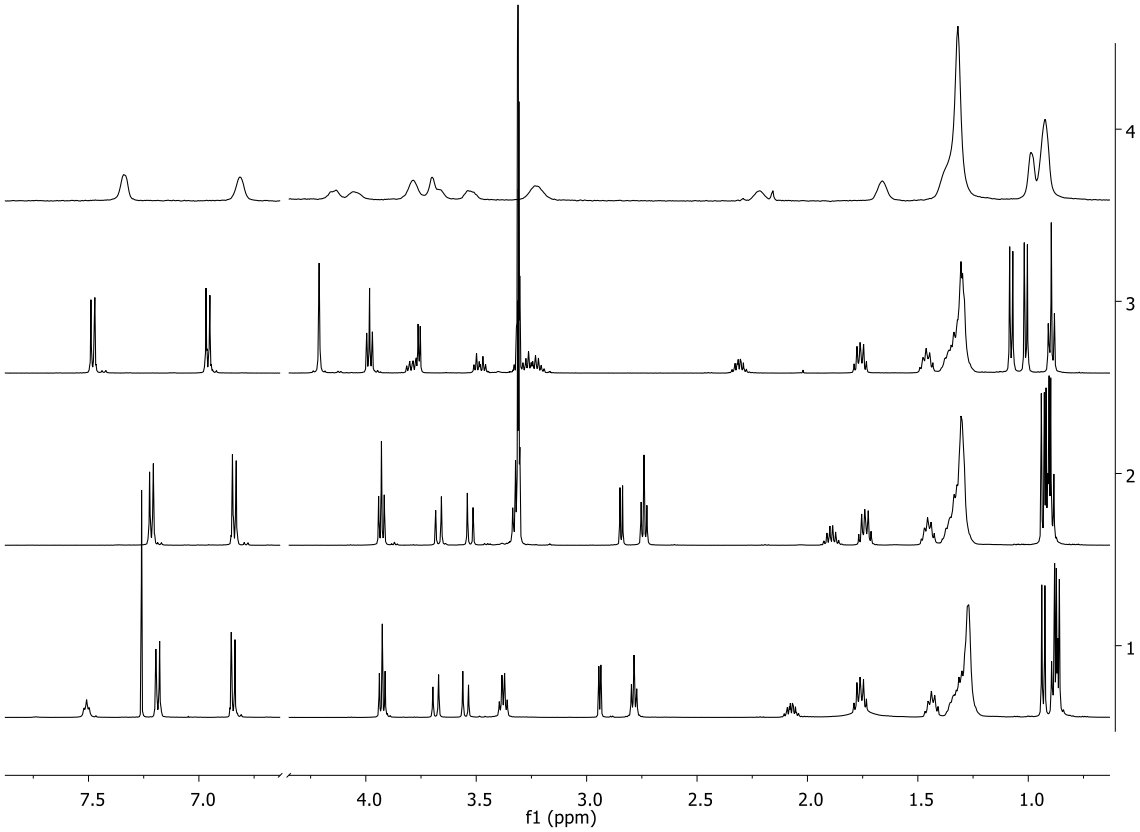

Figure S3. gNOESY spectrum of **1** (500 MHz, 3 mM in D_2O, 30 mM of trifluoroacetic acid, pH ~ 2-3, 298.15 K, mixing time = 200 ms). The spectrum shows very large and negative (with the same sign of the main diagonal) peaks for virtually all the proton signals. This observation implies the efficient spin diffusion and a slow tumbling time of the observable species in solution.

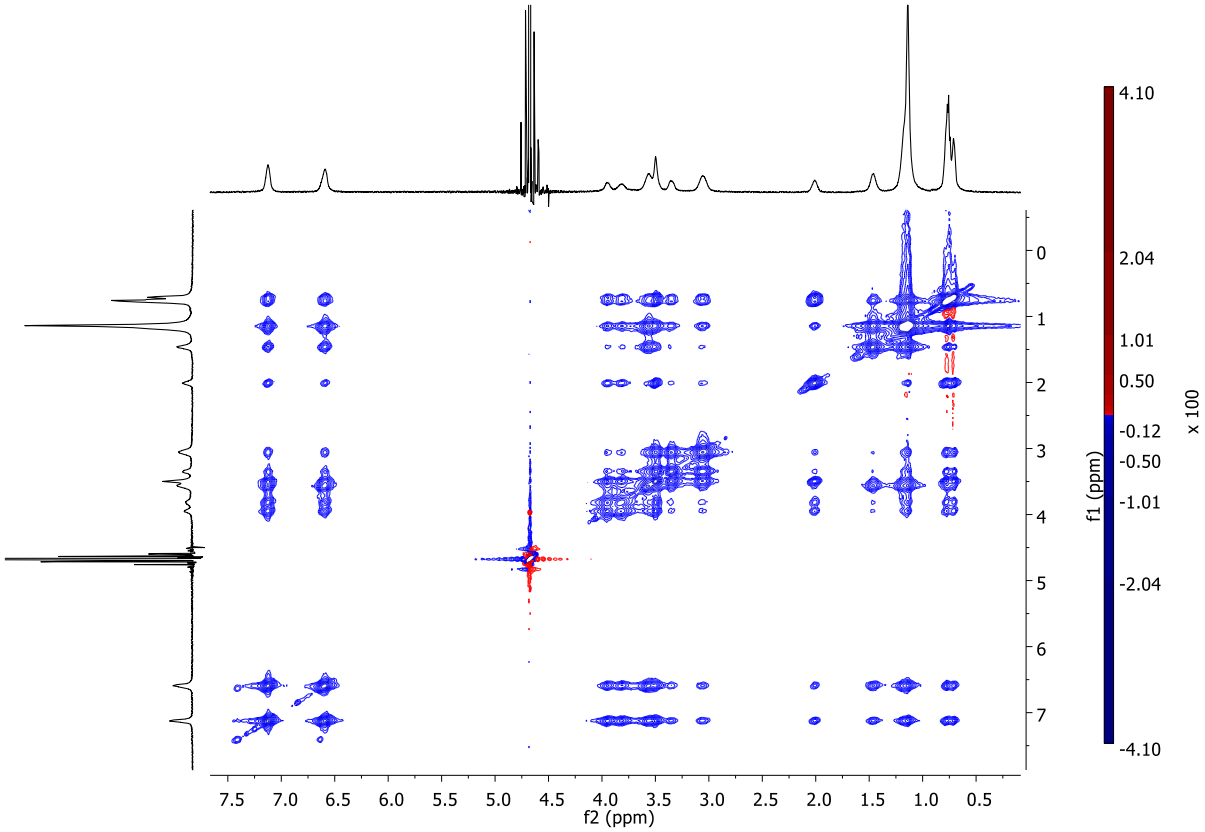

Figure S4. gROESY spectrum of **1** (500 MHz, 3 mM in D_2O, 30 mM of trifluoroacetic acid, pH ~ 2-3, 298.15 K, mixing time = 200 ms). The spectrum shows a small number of positive and weaker cross-peaks, since the ROESY experiments avoids spin diffusion and always shows positive effects (regardless the tumbling time of the species). This experiment confirms the observation of efficient spin diffusion in the NOESY experiment.

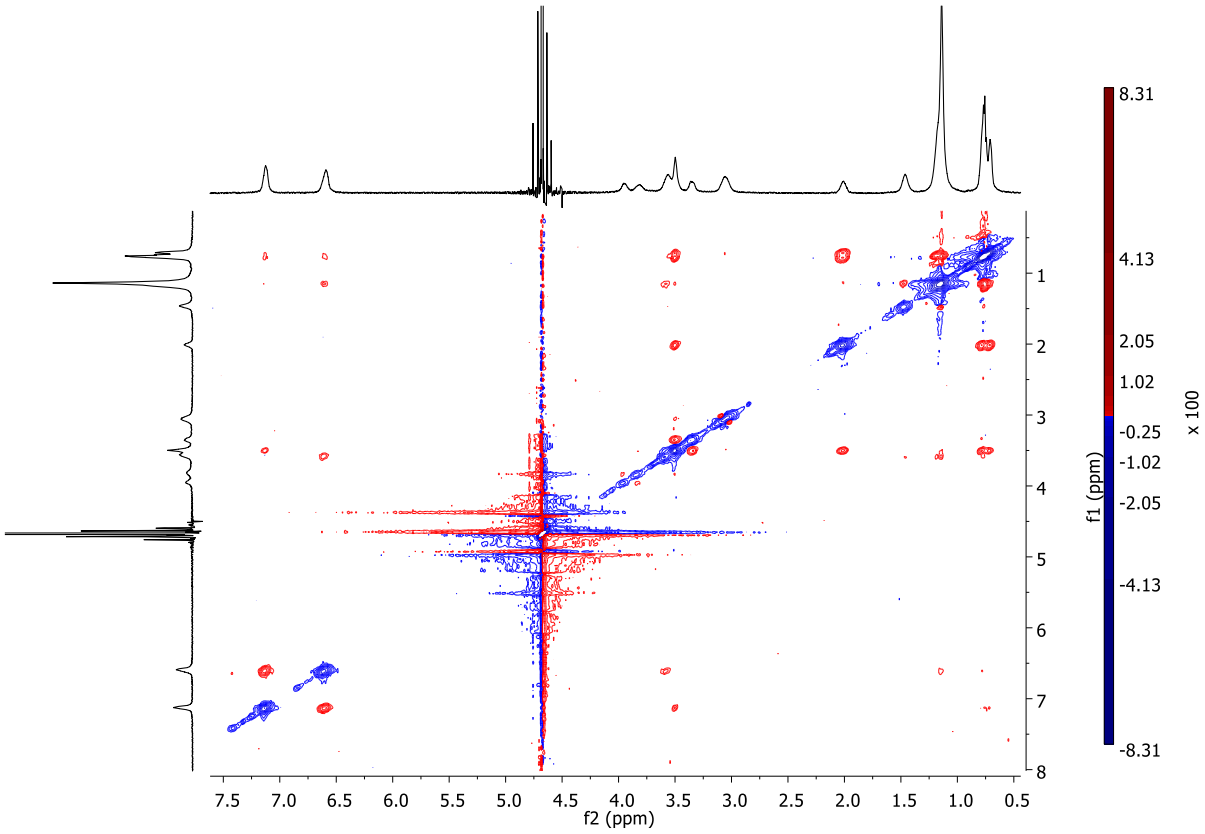

Figure S5. DOSY spectrum of **1** (500 MHz, 3 mM in D_2O, 30 mM of TFA, 298.15 K, Dbppste sequence, diffusion gradient length = 2.5 ms, diffusion delay = 300 ms, 60 increments for the array in the diffusion scale).

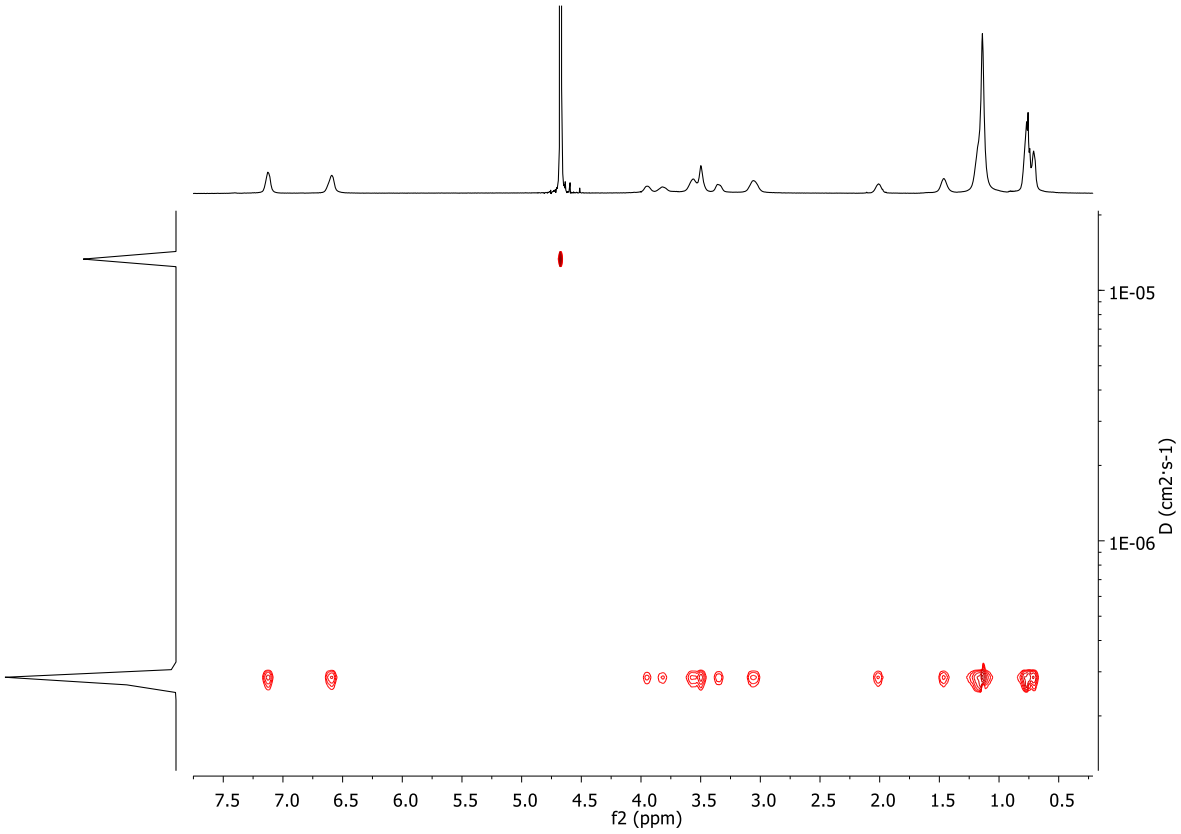

Considering the Stokes-Einstein equation for a spherical shape, the translational self-diffusion rate (D) can be expressed by the following equation:

$$D = \frac{k_B \cdot T}{6\pi \cdot \eta \cdot R_H}$$

where k_B is the Boltzmann constant ($1.3806504 \cdot 10^{-23}$ $J \cdot K^{-1}$), T is the absolute temperature, η is the viscosity of the medium ($1.096 \cdot 10^{-3}$ $J \cdot s \cdot m^{-1}$ for D_2O at 298.15 K, taken from Millero et al. *J. Chem. Eng. Data* 1971, vol. 16, 85-87) and R_H is the hydrodynamic radius. The NMR-measured D for **1** was $2.8 \pm 0.3 \cdot 10^{-7}$ $cm^2 \cdot s^{-1}$, which corresponds to an apparent R_H ~7.1 nm. Following, a structural proposal for the vesicular assembly in solution is shown:

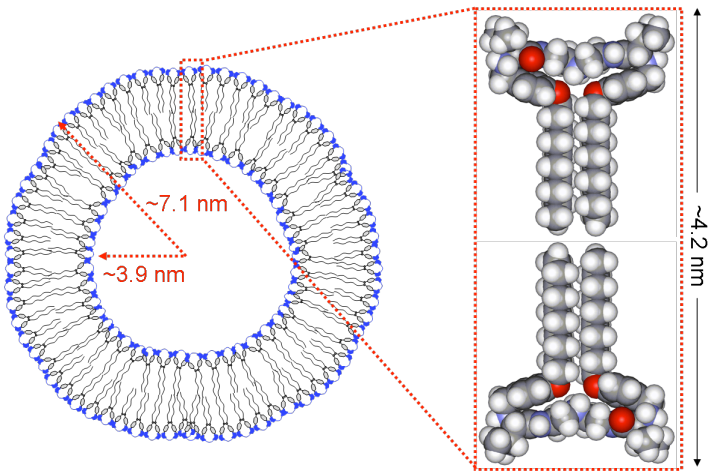

Figure S6. Change in the I_1/I_3 fluorescence ratio of pyrene as a function of the concentration of compound **1** at acidic pH (A) and at pH 7 (B).

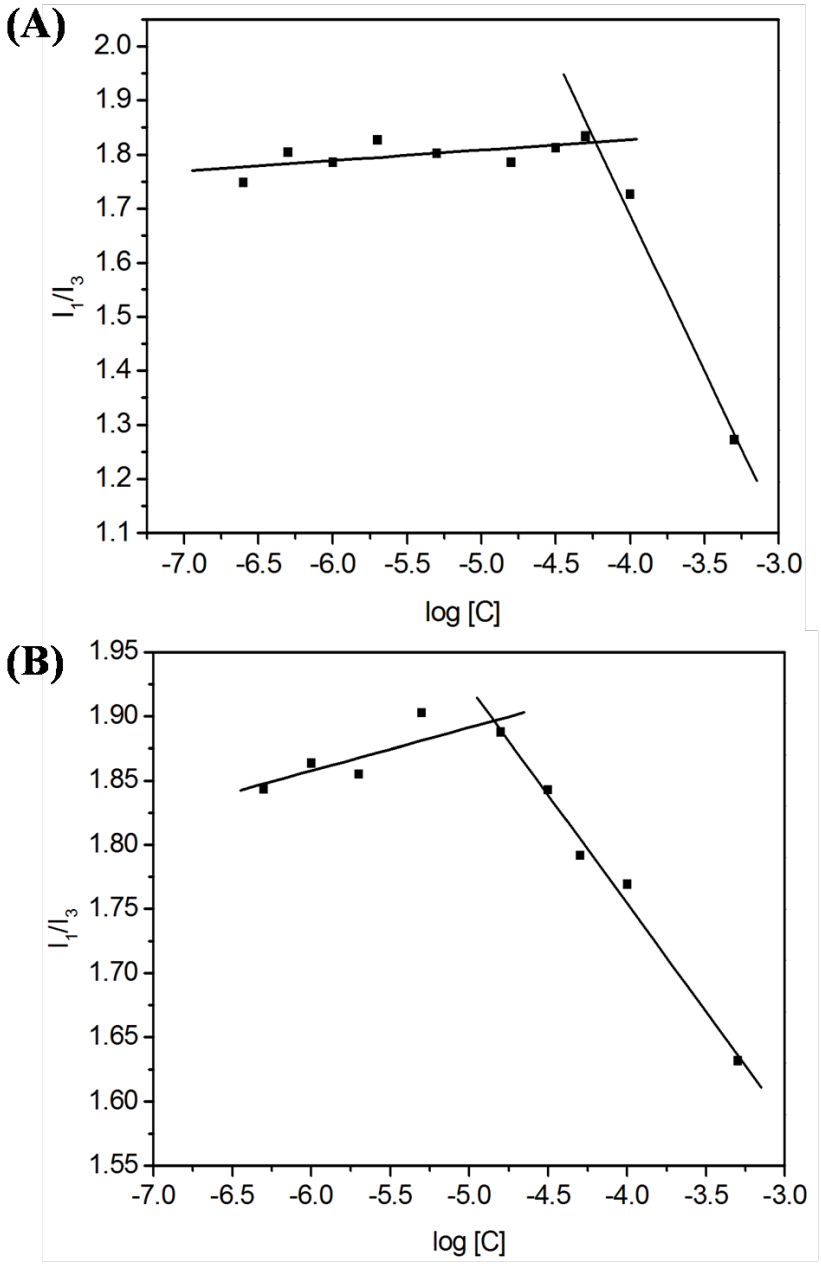

.

Figure S7. SEM micrographs of **1** grown from different media:
(A and B) $CHCl_3$
(C and D) MeOH
(E and F) 2 : 1 MeOH : H_2O
(G) 2 : 1 MeOH : H_2O + NaOH
(H and I) 2 : 1 MeOH : H_2O + HCl.
The corresponding scale bars are shown for every picture.

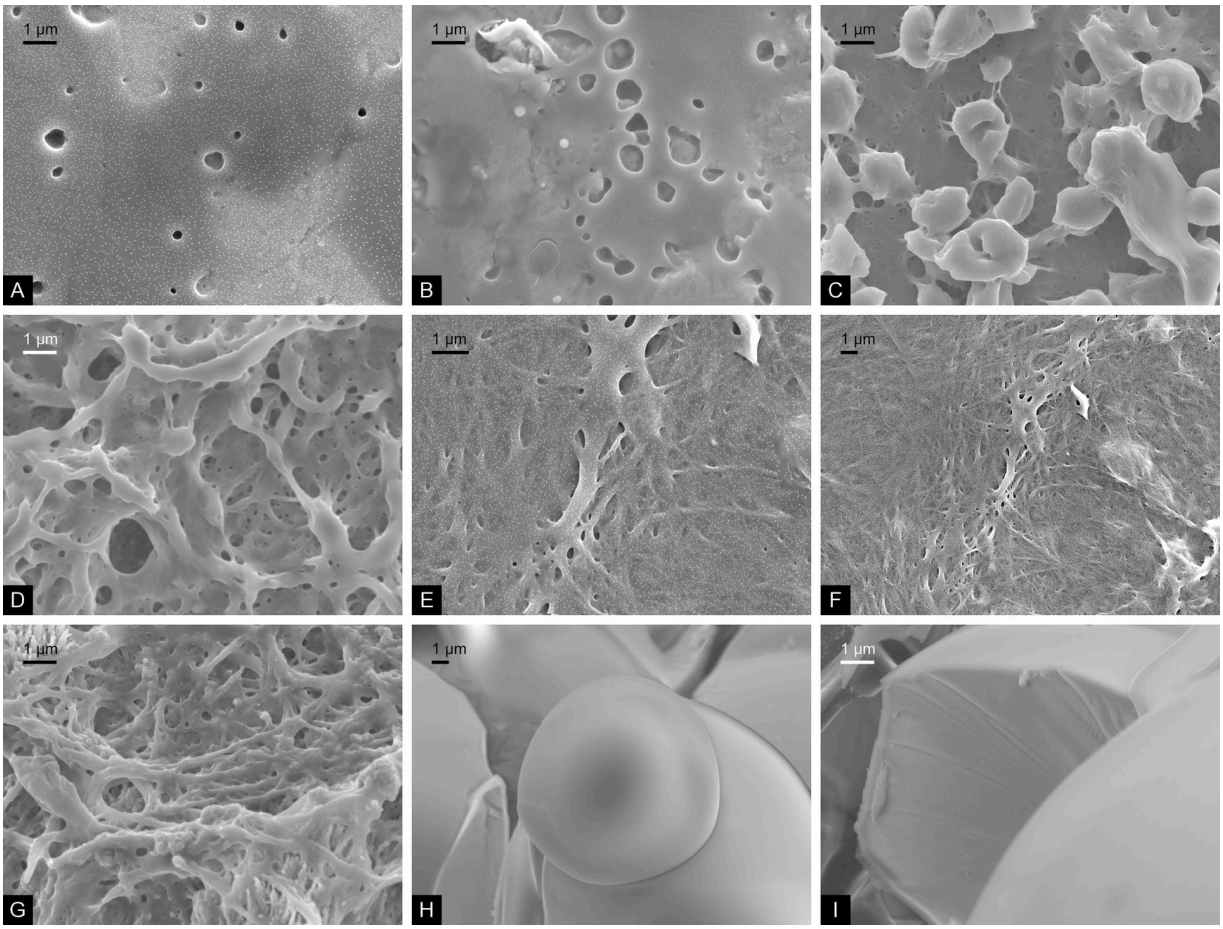

Figure S8. SEM micrographs of **1** grown from pure water at (A, B and C) neutral and (D, E and F) acidic pH values. The corresponding scale bars are shown for every picture.

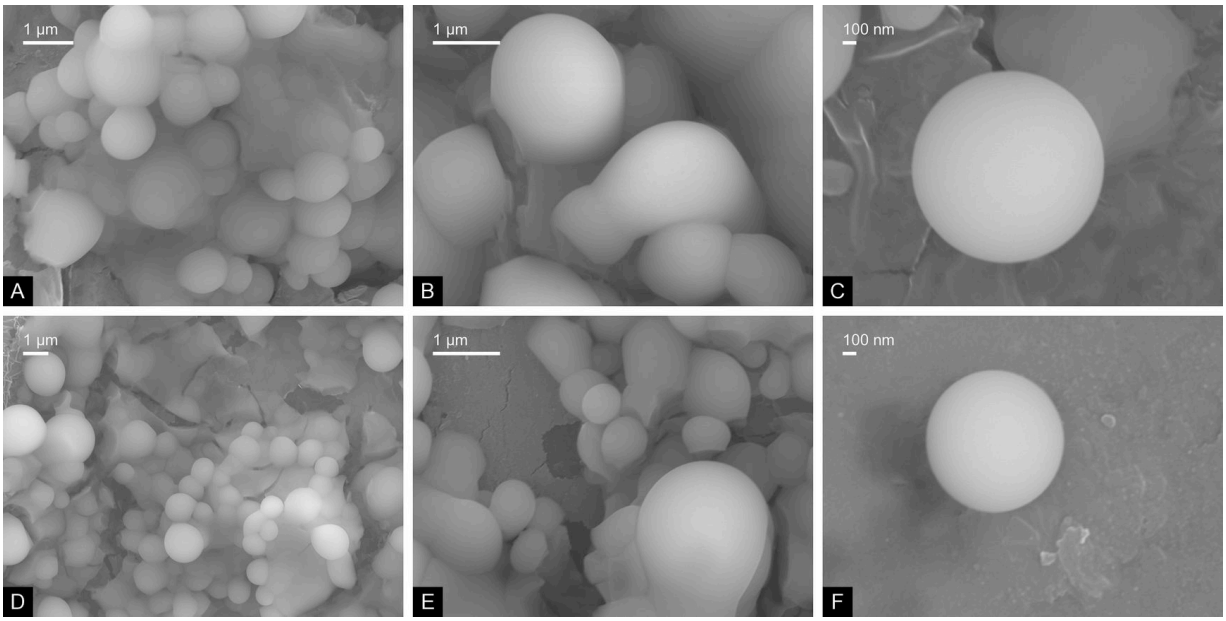

Figure S9. TEM micrographs of **1** grown from pure water at (A, B and C) neutral and (D, E and F) acidic pH values. The corresponding scale bars are shown for every picture.

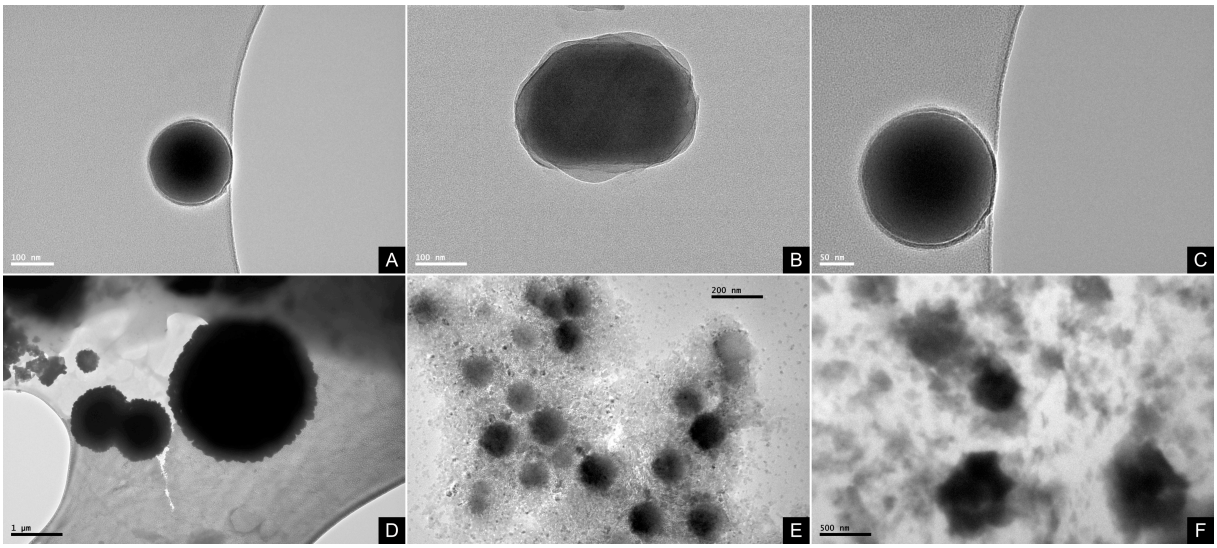

Figure S10. TEM micrographs of **1**:
(A and B) from 40 : 60 MeOH : H_2O, initially dissolving **1** in MeOH and then adding H_2O, leading to the formation of a gel.
(C, D, E and F) 60 : 40 H_2O : MeOH, initially dissolving **1** in H_2O and then adding MeOH, with no formation of a gel.
The corresponding scale bars are shown for every picture.

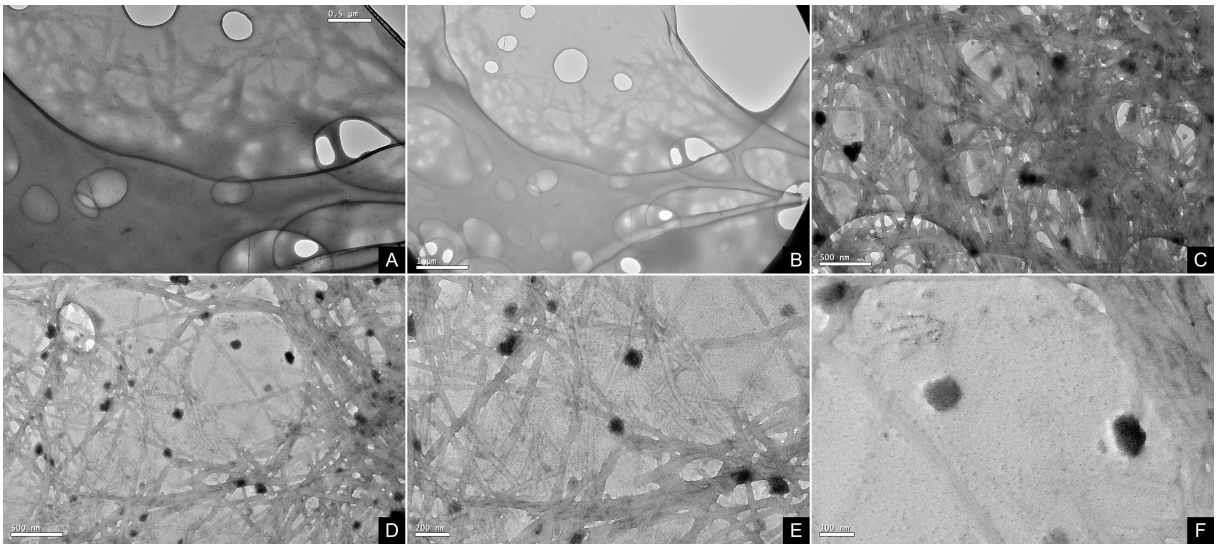

Table S1: ATR FT-IR data (cm^{-1}) of **1** in different media.

solvent	sample[a]	Amide A[b]	C-H stretch[b]	Amide I[b]	Amide II[b]
H_2O	1	3305 (b)	2924, 2852 (m)	1643 (b)	1544, 1510 (m)
	2	3307 (b)	2924, 2852 (m)	1643 (b)	1544, 1510 (m)
	3	3308 (m)	2924, 2852 (m)	1643 (b)	1544, 1510 (m)
	dry	3315 (m-s)	2920, 2851 (m-s)	1641 (m-s)	1545, 1510 (s)
H_2O/H^+	1	overlapped	2895 (b)	1645 (b)	1565, 1538 (m)
	2	overlapped	2928, 2855 (m)	1619 (b)	1565, 1538 (m)
	3	overlapped	2926, 2853 (m)	1619 (b)	1565, 1538 (m)
	dry	overlapped	2920, 2851 (m-s)	1641 (m-s)	1545, 1510 (s)
MeOH : H_2O	1	3407 (b)	3013, 2884 (b)	1647 (b)	1544, 1510 (m)
50 : 50	2	3289 (b-m)	2923, 2852 (m)	1647 (b-m)	1544, 1510 (m)
	3	3289 (b-m)	2921, 2852 (m)	1647 (b-m)	1544, 1510 (m)
	dry	3315 (m-s)	2920, 2851 (m-s)	1641 (m-s)	1545, 1510 (s)
MeOH : H_2O /H^+	1	overlapped	2983, 2895 (b)	1651 (b)	1541, 1508 (m)
50 : 50	2	overlapped	2983, 2895 (m)	1651 (b)	1541, 1508 (m)
	3	overlapped	2983, 2895 (s)	1651 (b)	1541, 1508 (m)
	dry	overlapped	2920, 2851 (m-s)	1641 (m-s)	1545, 1510 (s)

[a]Samples '1-3' correspond to acquisition at increasing concentrations obtained by the evaporation of the solvent, while 'dry' states for the solid sample. [b]The letter in parenthesis describes the shape of the band (b: broad, m: medium, s: sharp).

Figure S11. Selected regions of several ATR FT-IR spectra of **1** upon the evaporation of the solvent (1-3-dried): (A) amide A, (B) amide I, (C) amide II, and (D) CH stretching in H_2O.

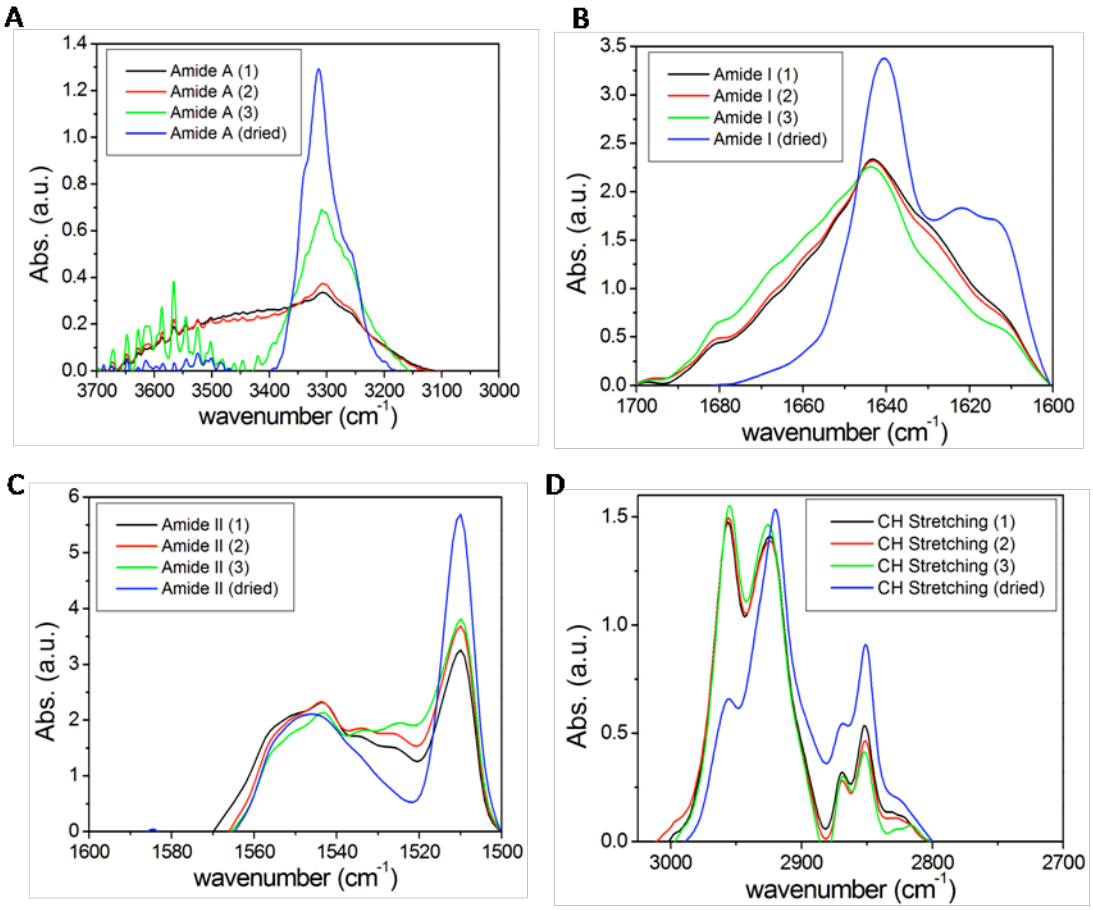

Figure S12. Selected regions of several ATR FT-IR spectra of **1** upon the evaporation of the solvent (1-3-dried): (A) amide I, (B) amide II, and (C) CH stretching in H_2O with acid.

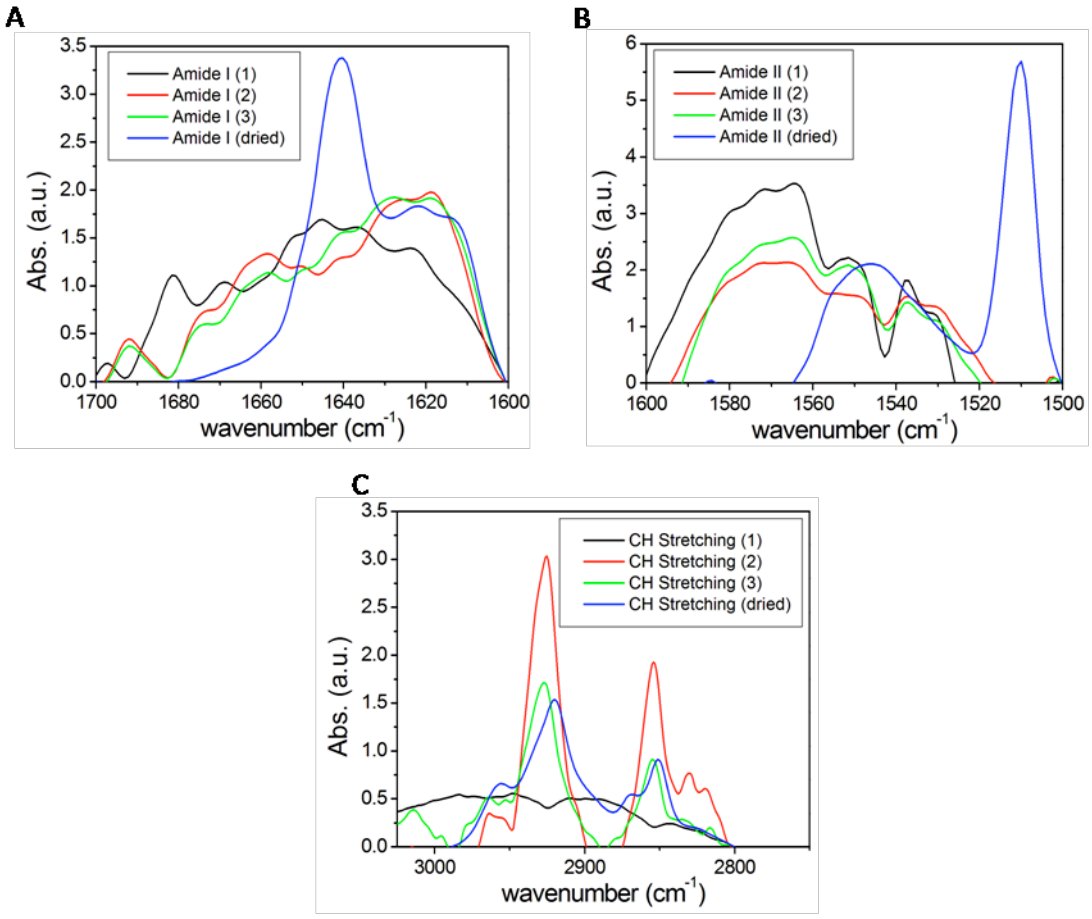

Figure S13. Selected regions of several ATR FT-IR spectra of **1** upon the evaporation of the solvent (1-3-dried): (A) amide A, (B) amide I, (C) amide II, and (D) CH stretching in 50 : 50MeOH : H_2O.

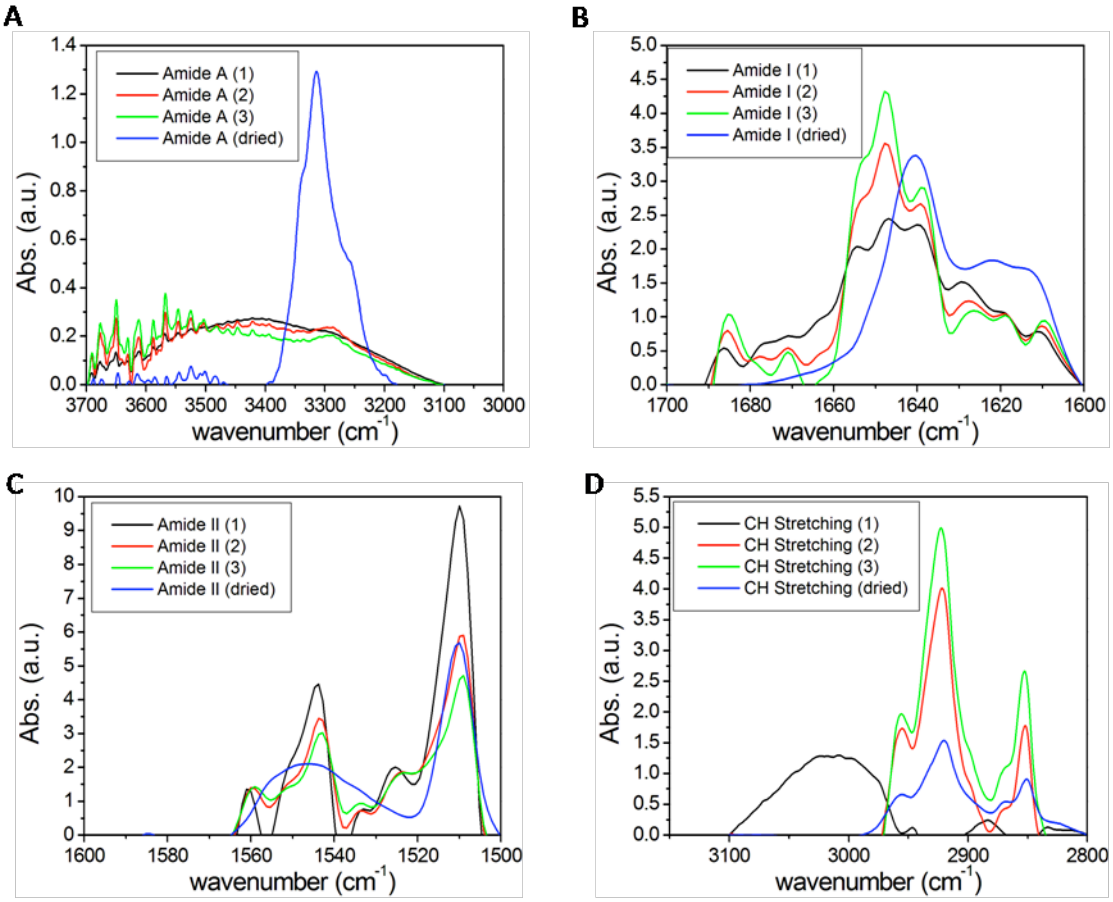

Figure S14. Selected regions of several ATR FT-IR spectra of **1** upon the evaporation of the solvent (1-3-dried): (A) amide I, (B) amide II, and (C) CH stretching in 50 : 50 MeOH : H_2O with acid.

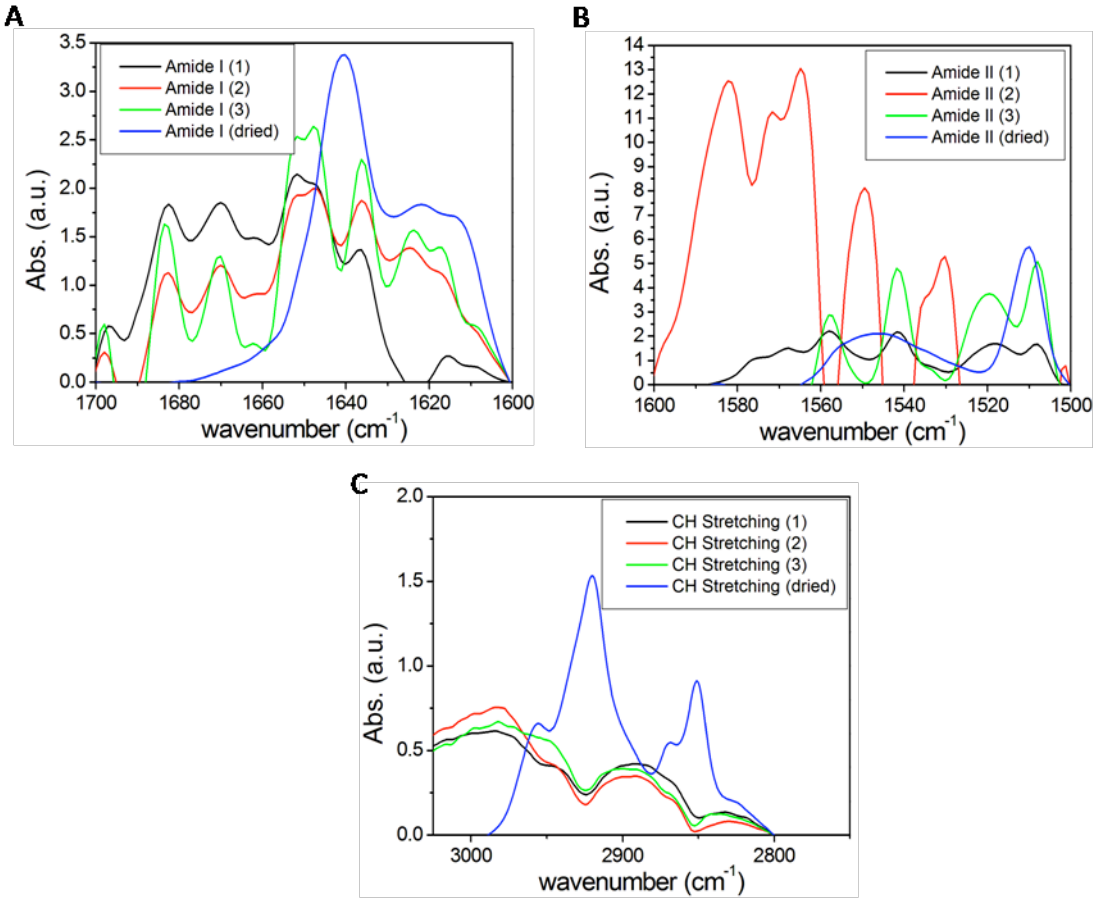

Figure S15. Schematic representation for the procedure for the formation of a stable gel at room temperature.

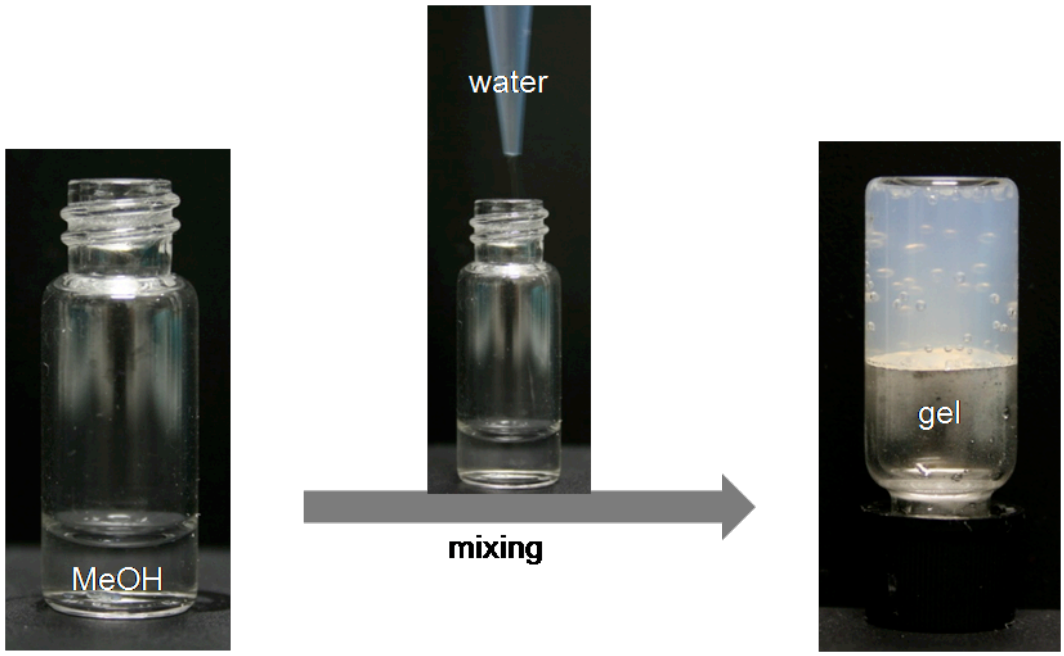

Figure S16. Photographs of the gels formed by **1** in 60:40 MeOH : H_2O using: (A) 0.25% weight, (B) 0.5% weight, (C) 1.0% weight, (D) 1.5% weight, and (E) 2.0% weight.

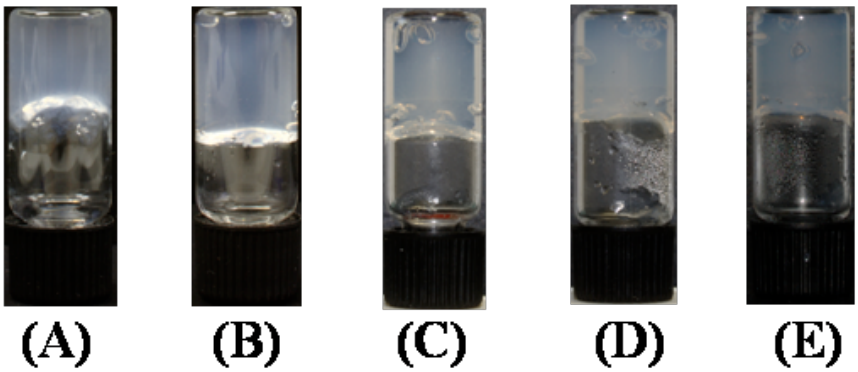

Figure S17. Photographs of the gels formed by **1** in 40:60 MeOH : H_2O using: (A) 0.25% weight, (B) 0.5% weight, (C) 1.0% weight, (D) 1.5% weight, and (E) 2.0% weight.

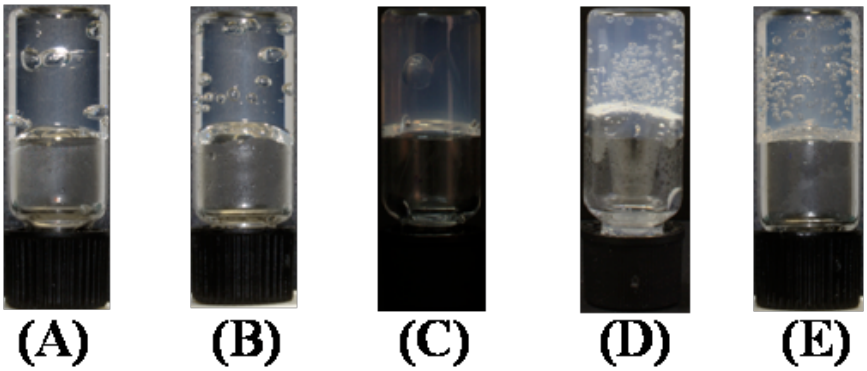

Figure S18. Photographs of the gels formed by **1** in 20:80MeOH : H_2O using: (A) 0.5% weight, (B) 1.0% weight, (C) 1.5% weight, and (D) 2.0% weight.

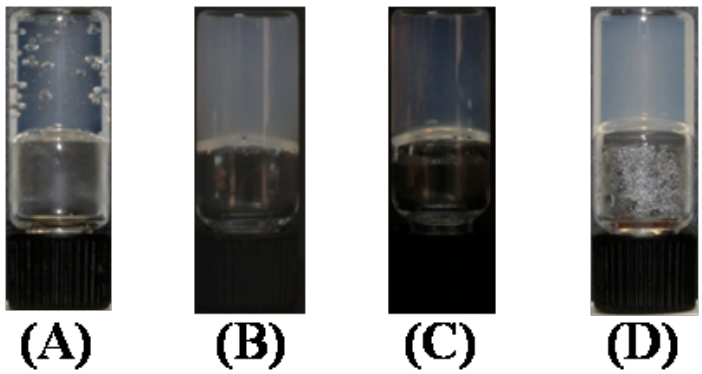

Figure S19. Photographs of the gels formed by **1** at 0.5% weight in: (A) 60 : 40 MeOH : H_2O, (B) 50 : 50 MeOH : H_2O, (C) 40 : 60 MeOH : H_2O, (D) 30 : 70 MeOH : H_2O, (E) 20 : 80 MeOH : H_2O, and (F) 10 : 90 MeOH : H_2O.

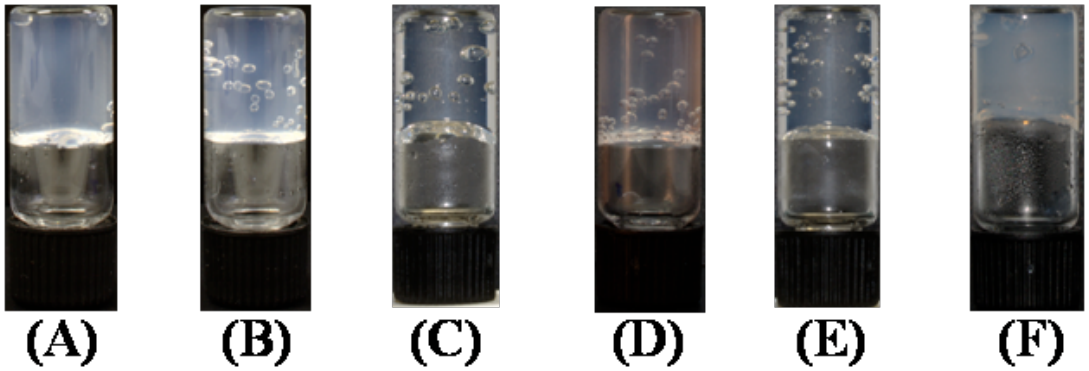

Figure S20. Photographs of the gels formed by **1** at 2.0% weight in (A) 60 : 40 MeOH : H_2O, (B) 50 : 50 MeOH : H_2O, (C) 40 : 60 MeOH : H_2O, (D) 30 : 70 MeOH : H_2O, (E) 20 : 80 MeOH : H_2O, and (F) 10 : 90 MeOH : H_2O.

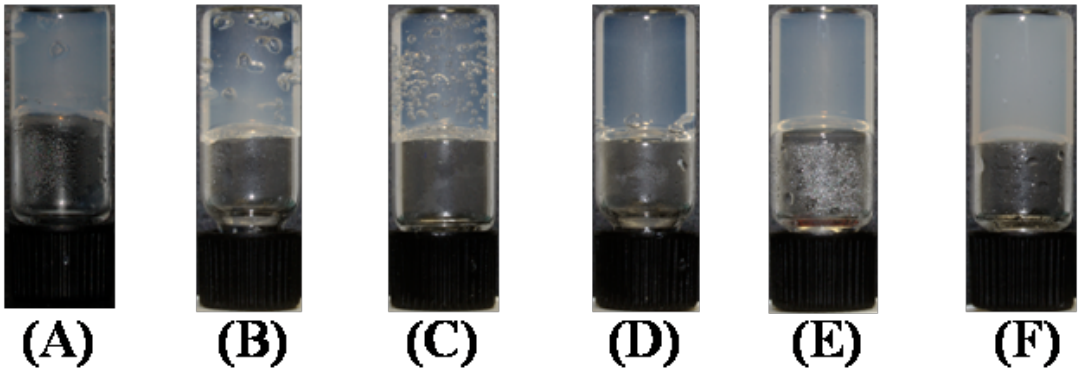

Figure S21. Snapshots of the acid-induced disassembly of the gel formed by **1**

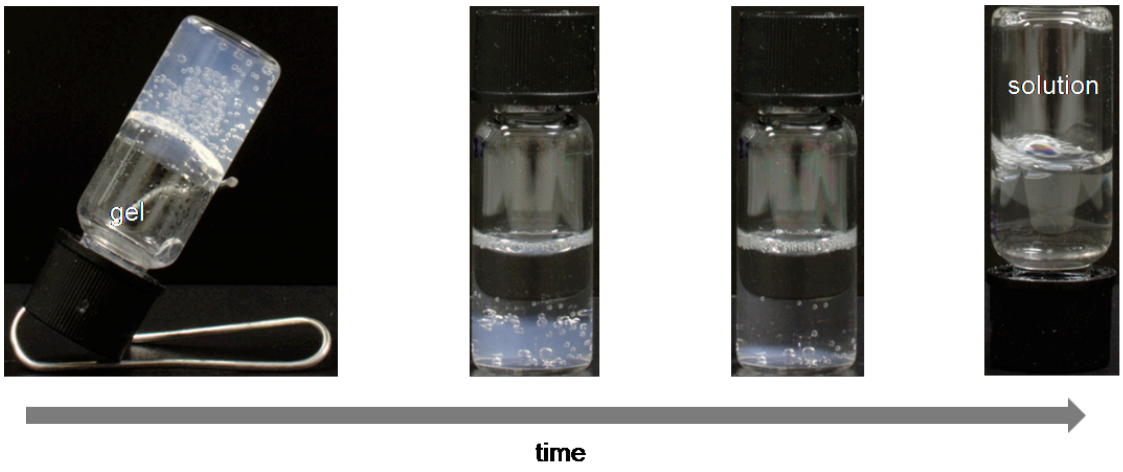

Figure S22. Photographs of the gels formed by 1% wt of **1** in (A) 40 : 60 EtOH : H_2O, (B) 20 : 80 EtOH : H_2O, and (C) 10 : 90 EtOH : H_2O.

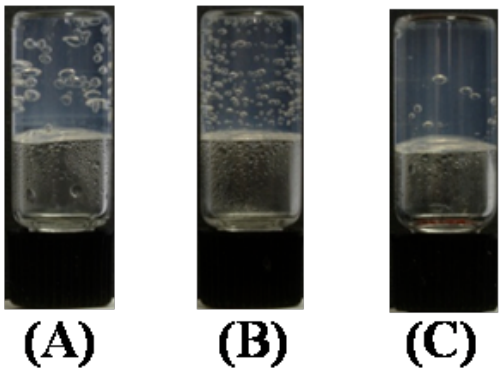

Table S2: Temperatures of gel disassembly as a function of solvent proportion. The gel was formed by 1% wt of **1**.

	EtOH : H_2O	Temperature of gel decomposition (ºC)	Photograph Fig S22
1	40 : 60	35.5 – 42.0	A
2	20 : 80	42.4 – 50.2	B
3	10 : 90	42.6 – 53.0	C

Figure S23. Temporal stability of hydrogels